2.A.1:
2.L

Nuclear Physics **50** (1964) 629—640; © *North-Holland Publishing Co., Amsterdam*

THE SCATTERING OF He^3 BY He^4

A. C. L. BARNARD, C. M. JONES † and G. C. PHILLIPS
Bonner Nuclear Laboratories, Rice University, Houston, Texas ††

Received 22 July 1963

Abstract: Cross sections for the elastic scattering of He^3 by He^4 have been measured for incident He^3 energies in the range $2.5 \leqq E_{He^3} \leqq 5.7$ MeV (lab system) using a Van de Graaff accelerator and a differentially pumped gas scattering chamber. Excitation functions were measured at centre-of-mass angles 54°44′, 63°27′, 73°,57′, 90°2′, 104°38′, 106°36′, 116°37′, 125°19′ and 140°50′. Angular distributions were measured at $E_{He^3} = 2.467$, 3.600, 4.761 and 5.703 MeV. The scattering phase shifts were obtained from these data. The general trend of the S-wave phase shift with energy is similar to that for hard-sphere scattering with a radius $R = 2.8$ fm, although there is some indication of a systematic departure from this. The variation of the δ_1^+ phase shift with energy is consistent with the effect of the Be^7 ground state, calculated using single-level dispersion theory. However, the behaviour of the δ_1^- phase shift cannot be explained by the effect of only the Be^7 first excited state. The presence of the second excited state in Be^7 explains the behaviour of the δ_3^+ phase shift fairly well. The parameters used for this state were $J^\pi = \frac{7}{2}^-$, $R = 4.4$ fm, characteristic energy = 3.56 MeV, reduced width = 0.7 MeV.

1. Introduction

Tombrello and Parker [1]) have recently published cross sections and phase shifts for the scattering of He^3 by He^4, for incident He^3 energies from 6 to 12 MeV and have also summarized theoretical work on the Be^7 nucleus. The level structure of this nucleus is shown in fig. 1. In an earlier experiment, Miller and Phillips [2]) investigated this scattering at lower energies. The use of scintillation detectors by Miller and Phillips led to some difficulties. At forward angles the scattered He^3 and the recoil He^4 particle groups were sufficiently close in energy that they could not be satisfactorily resolved using pulse-height analysis alone. At backward angles the scattered He^3 particles have very low energies, and the pulses produced by them in the scintillation detector were little larger than the noise.

The present experiment covered the energy range $2.5 \leqq E_{He^3} \leqq 5.7$ MeV and essentially repeated the measurements of Miller and Phillips, using improved experimental techniques. In particular, the use of silicon surface barrier detectors greatly reduced both of the difficulties mentioned above.

Two sets of phase shifts were obtained from the measured cross sections. The two sets differ principally in the sign of the splitting of the P-wave phase shifts and they

† Now at the Oak Ridge National Laboratory, Oak Ridge, Tennessee.
†† Work supported in part by the U. S. Atomic Energy Commission.

consequently predict opposite spin polarizations in certain energy-angle regions. The "set B" phase shifts, which have δ_1^+ larger (closer to 180°) than δ_1^-, are preferred on the basis of the continuity of phase shifts as a function of energy. This P-wave splitting is opposite to that used by Miller and Phillips [2]) and by Tombrello and Parker [1]).

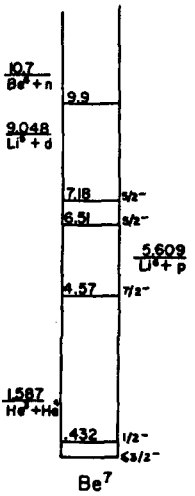

Fig. 1. Energy levels in Be^7.

2. Measurement of Cross Sections

A type CN Van de Graaff accelerator was the source of He^3 particles. The beam entered the differentially-pumped precision gas scattering chamber described by Jones *et al.*[3]), equipped for this experiment with two ORTEC silicon surface-barrier detectors. The experimental methods were generally similar to those described for a $p+He^4$ scattering experiment by Barnard, Jones and Weil [4]). In addition, in the present experiment is was necessary to determine the mean charge state of the particles entering the Faraday cup, and to take careful account of the inhomogeneity of the field of the 90° analysing magnet, caused by magnetic saturation, which affected the energy calibration.

The mean charge state was measured by scattering He^3 particles from natural argon. Since the barrier height here is approximately 10 MeV, scattering of He^3 in the present energy range is expected to follow the Rutherford form closely. Apparent cross sections were measured at $\theta_{c.m.} = 56°45'$ for 16 He^3 energies from 2.4 to 3.9 MeV, with the assumption that all particles entering the Faraday cup were doubly charged. The ratio of the apparent cross section to the Rutherford cross section was taken as a measure of the mean charge state. This ratio differed significantly from unity only in the lowest part of the He^3 energy range used. At 2.5 MeV the average value was 1.025, whereas for the nine measurements above 3 MeV, the ratio averaged 1.011 ± 0.020 for one detector and 0.997 ± 0.014 for the other.

Except where the yield was particularly small, the counting statistics were better than ± 3% and the overall accuracy of the cross sections is estimated as better than ± 5%.

The energy calibration for the experiment was provided by absolute measurements of the energy of He^3 particles elastically scattered from gold. These measurements were made at eight different settings of the 90° analysing magnet, using the 180° magnetic spectrometer described by Famularo and Phillips [5]). Table 1 shows the energy compu-

TABLE 1
Incident energy computation

Kf^2 MeV	ΔE_{sat} MeV	ΔE_{dp} (MeV)	E_{targ} (MeV)	Estimated accuracy (keV)
2.989	0.014	0.014	2.961	±20
3.690	0.047	0.025	3.618	±20
5.138	0.158	0.021	4.959	±40
5.996	0.253	0.019	5.724	±40

tation at various incident energies. In the absence of any inhomogeneity of the field of the 90° analysing magnet and neglecting relativistic effects, the particle energy would be $E = kf^2$. Here k is a constant determined by geometry and f is the NMR magnetometer frequency. From this value ΔE_{sat} is subtracted to account for the field inhomogeneity produced by saturation. The particles then lose an amount of energy ΔE_{dp} in passing through the differential pumping system [3]) before reaching the target. As shown in table 1, the energy scale for this experiment is estimated to be accurate to ±20 keV below 4 MeV and ±40 keV above that energy. These values are also consistent with the Rutherford scattering measurements mentioned above, since at 4 MeV a 20 keV error produces a 1% change in the Rutherford cross section.

3. Cross Sections

Fig. 2 shows excitation functions at centre-of-mass angles $\theta_{c.m.}$ = 54°44′(R), 63°27′, 73°57′(R), 90°2′, 104°38′, 116°37′, 125′19′, 140′50′ respectively. Here (R) indicates cross sections obtained from recoil He^4 groups. The anomaly seen in the excitation functions is due to the second excited state in Be^7 (see fig. 1). Note that at $\theta_{c.m}$ = 63°27′ the cross section almost vanishes at about 5.24 MeV. The energy scales for different excitation functions may differ by approximately ±20 keV because of the imperfect reproducibility of the 90° magnet inhomogeneity. In cases when the measurement of an excitation function was interrupted, corrections of this order of magnitude were made when necessary to force agreement between the repeated parts of the function. Fig. 3 shows angular distributions measured at energies E_{He^3} = 2.467, 3.600, 4.761 and 5.703 MeV. The cross section at $\theta_{c.m.}$ = 54°44′, 73°57′, 84°12′ and 106°36′ were obtained from recoil He^4 groups and are seen to be consistent with the data at other angles, obtained from the He^3 groups. The angular distribution cross sections are also shown in fig. 2, where they are indicated by crosses.

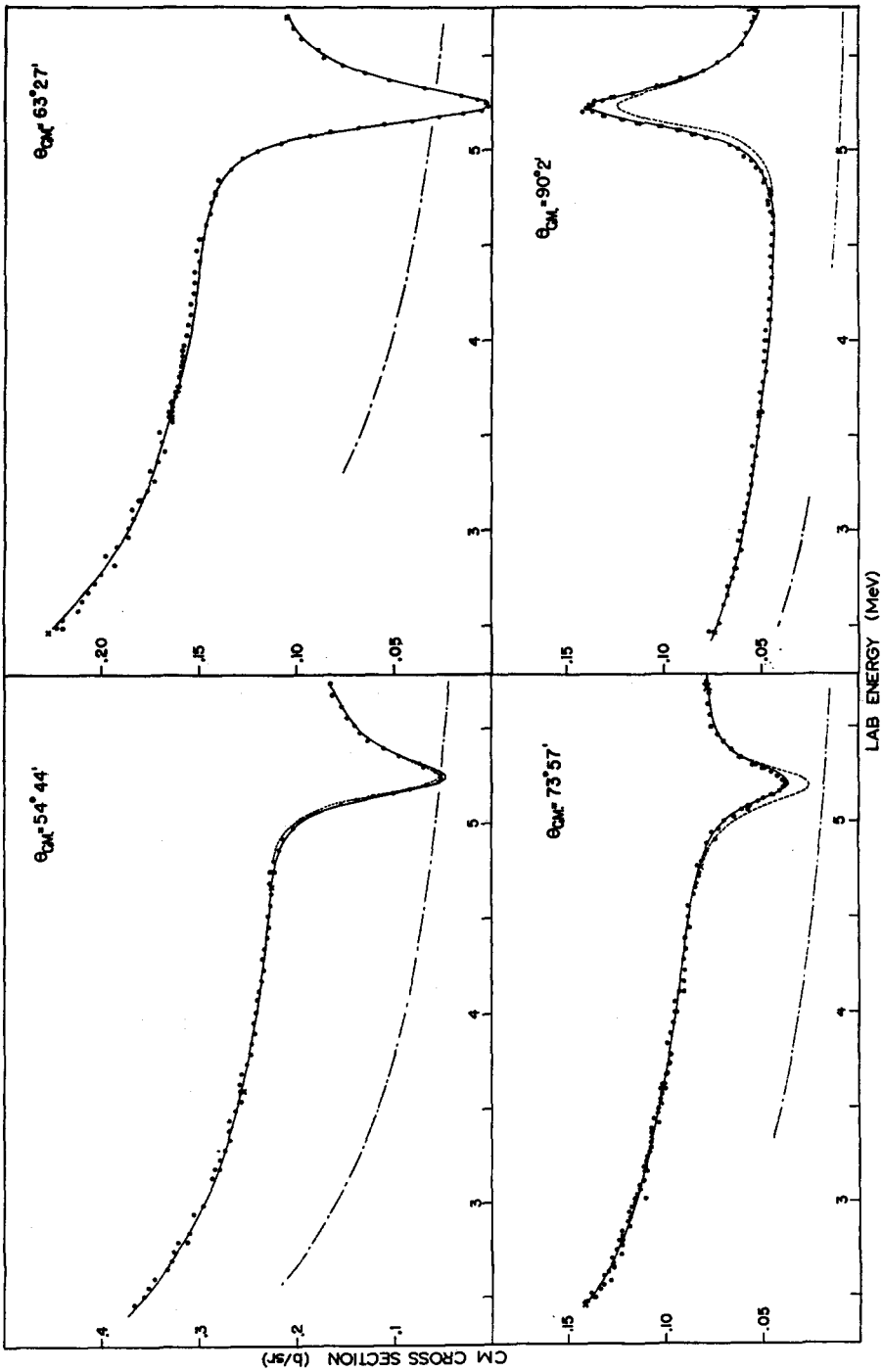
θCM=63°27'
θCM=90°2'
θCM=54°44'
θCM=73°57'
CM CROSS SECTION (b/sr)
LAB ENERGY (MeV)

Fig. 2(a).

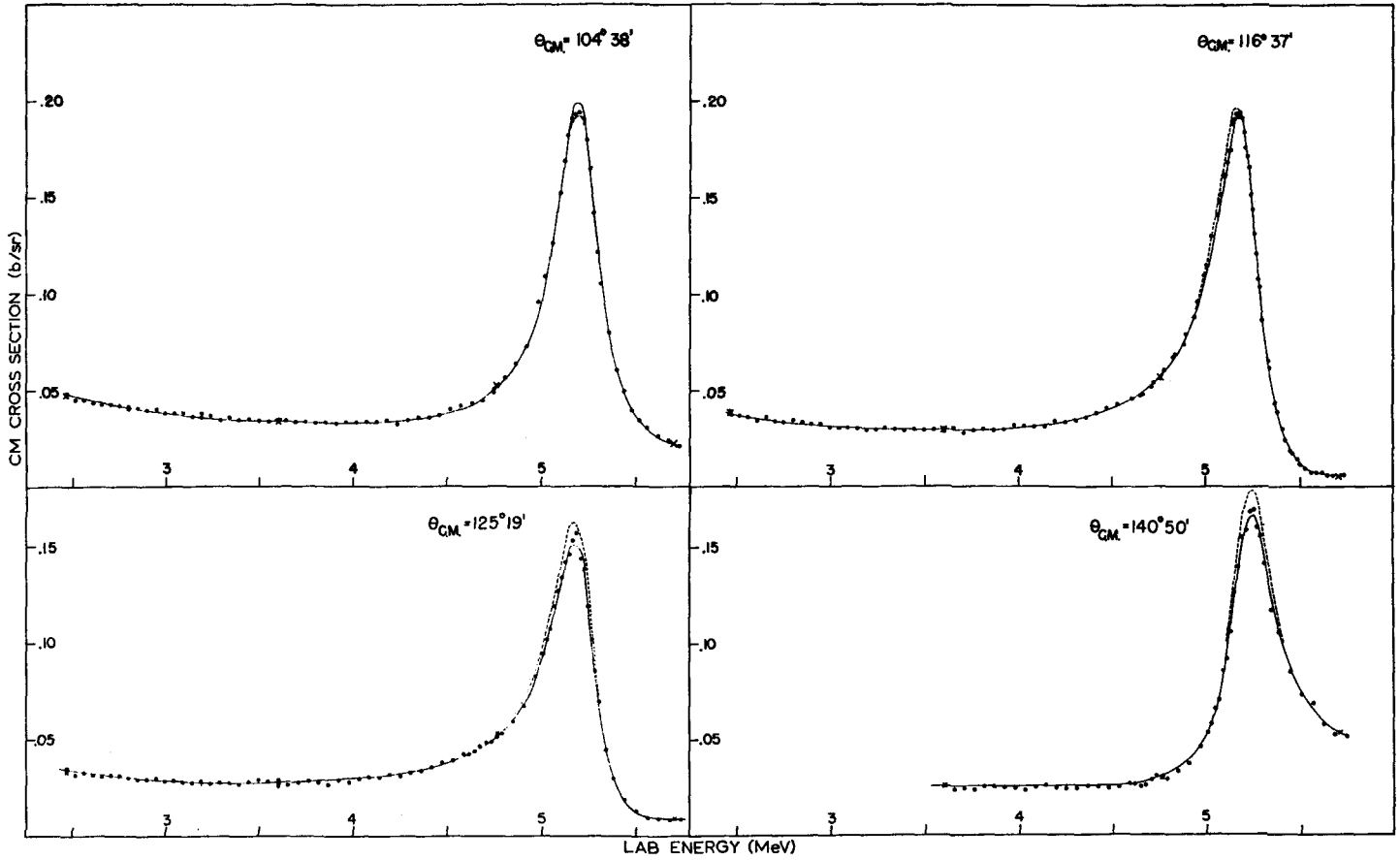

Fig. 2(b). Excitation function for scattering of He^3 by He^4 at the centre-of-mass angle indicated. Solid and short dash curves are calculated from the phase shifts. The dash-dot curve is the Rutherford scattering cross section. The circles are the experimental points and the crosses are the points from angular distributions.

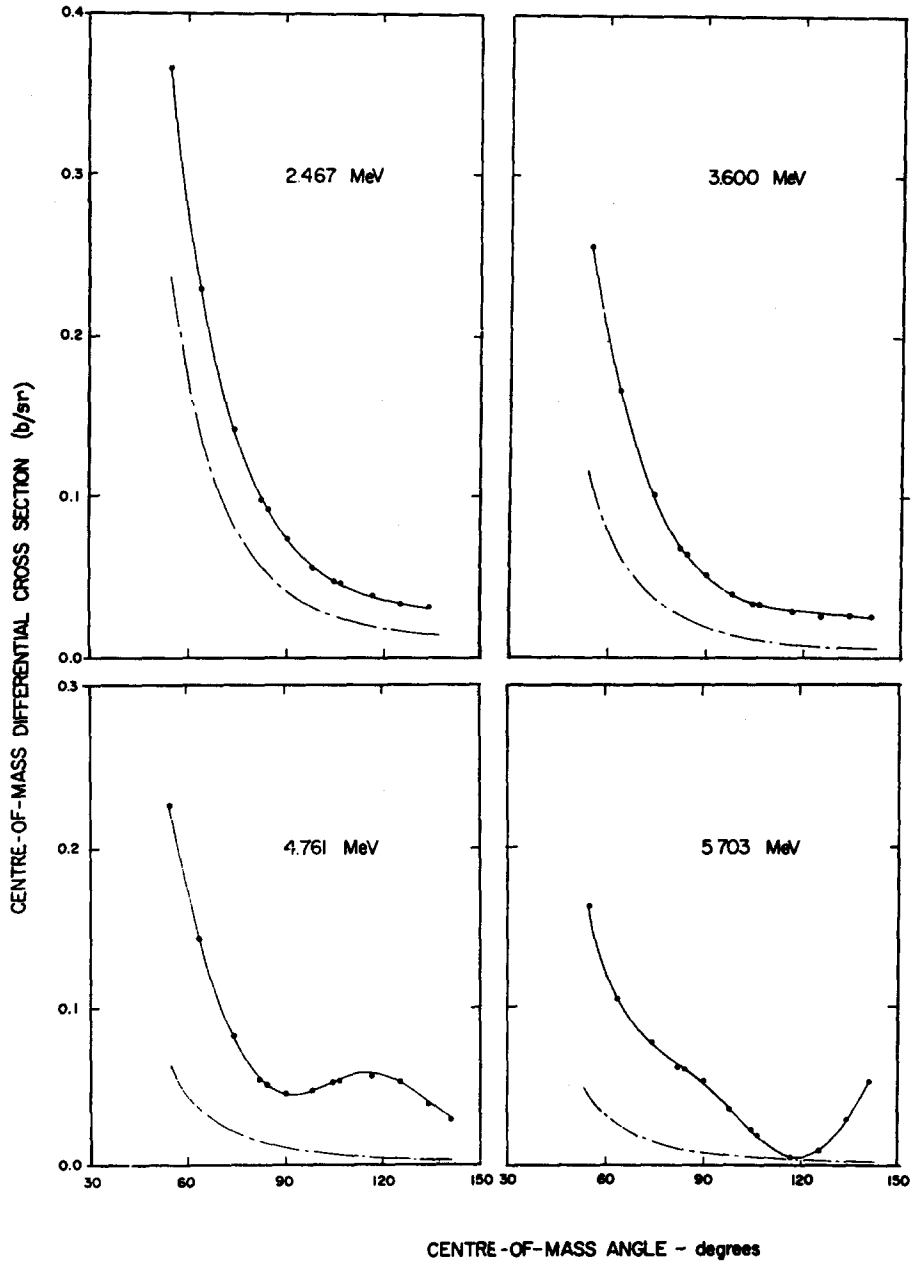

Fig. 3. Angular distributions for scattering of He^3 by He^4 at the incident He^3 energies stated. Solid curves are calculated from the phase shifts. The dash-dot curves are Rutherford scattering cross sections.

4. Phase Shifts

The experimental phase shifts were obtained using the IBM 1401 computer installed "on site" in the Bonner Nuclear Laboratories. Method B described by Barnard, Jones and Weil [4]) was used. Since no D-wave levels have been identified in Be^7, the D-wave phase shifts were held at their hard-sphere values for a radius of about 3 fm.

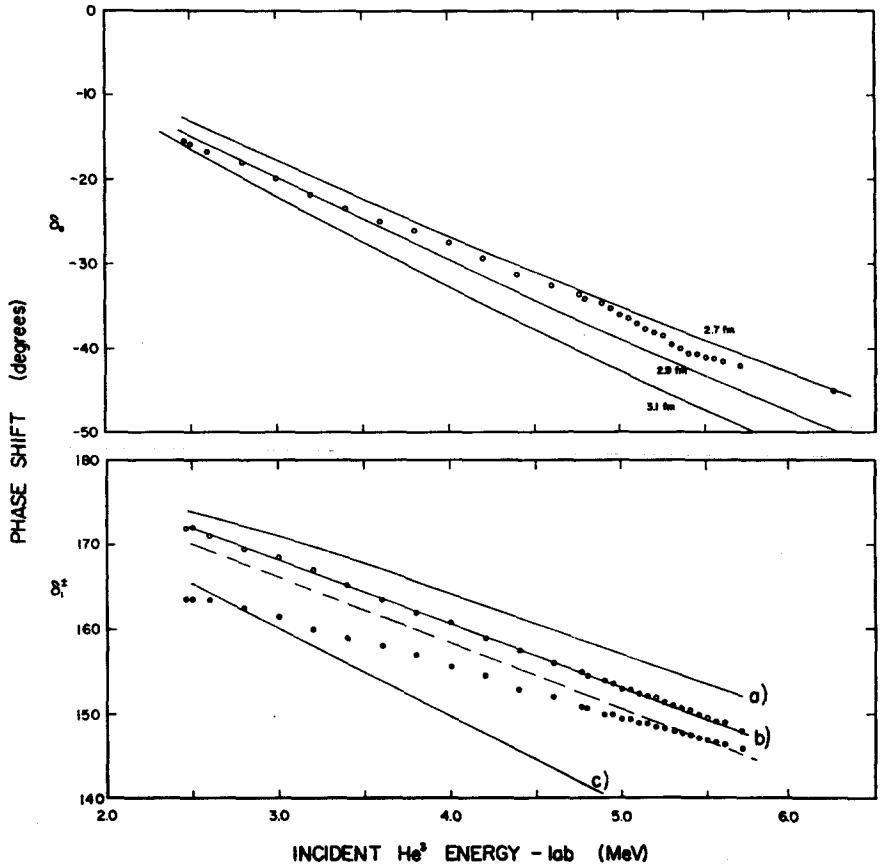

Fig. 4 (upper). Open circles are experimental S-wave phase shifts of set B. Solid curves are hard-sphere scattering phase shifts calculated for radii indicated. The open circles are the present data, and the closed circles are the data of ref.[1]). (lower) Open circles are experimental δ_1^+ phase shifts, closed circles are experimental δ_1^- phase shifts of set B. Solid curves are calculated for $R = 3.8$ fm. Curve (a) is for hard-sphere scattering (with 180° added). Curve (b) is δ_1^+ calculated for $\theta_{gs}^2 = 0.15$. Curve (c) is δ_1^- calculated for $\theta_1^2 = 1.0$. The dashed curve is δ_1^- calculated for $R = 2.8$ fm, $\theta_1^2 = 2.0$.

The phase shifts for $l \geqq 4$ were set to zero. Thus the adjustable parameters were the S-, P- and F-wave phase shifts. Since P- and F-wave levels are known in Be^7 (see fig. 1) no attempt was made to fit the data with these phase shifts unsplit. The first efforts in the phase shift analysis were directed towards obtaining a set of phase shifts, which

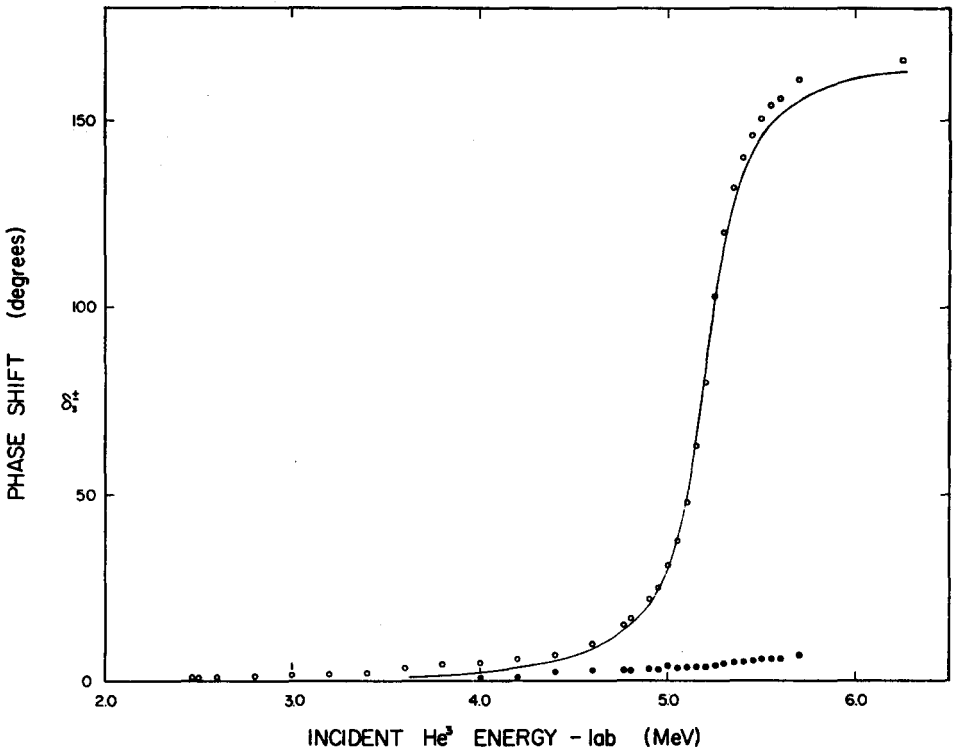

Fig. 5. Open circles are experimental $\delta_3{}^+$ phase shifts, closed circles are experimental $\delta_3{}^-$ phase shifts of set B. The square is the $\delta_3{}^+$ phase shift of ref.[1]), and the triangle is the $\delta_3{}^-$ phase shift of ref.[1]). The solid curve is $\delta_3{}^+$ calculated for $R = 4.4$ fm, $\theta_3{}^2 = 0.38$ and $E_x = 4.57$ MeV.

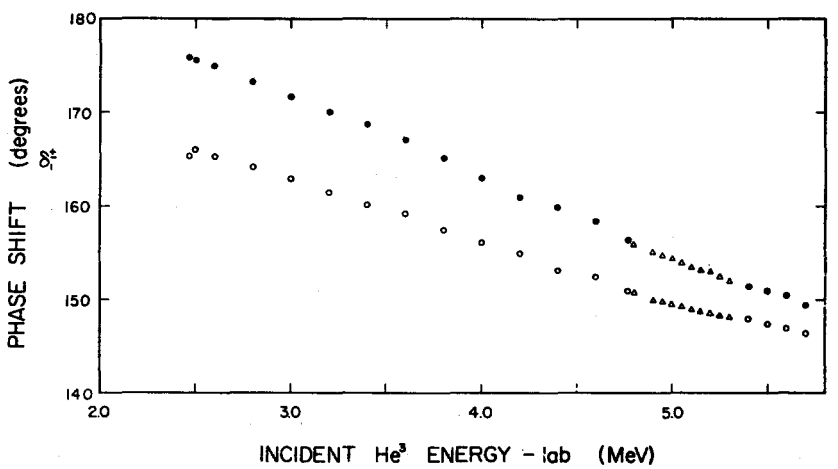

Fig. 6. P-wave phase shifts of set A. The open and closed circles are the $\delta_1{}^+$ and δ_1 phase shifts for a good fit to the data. The triangles are the interpolated values.

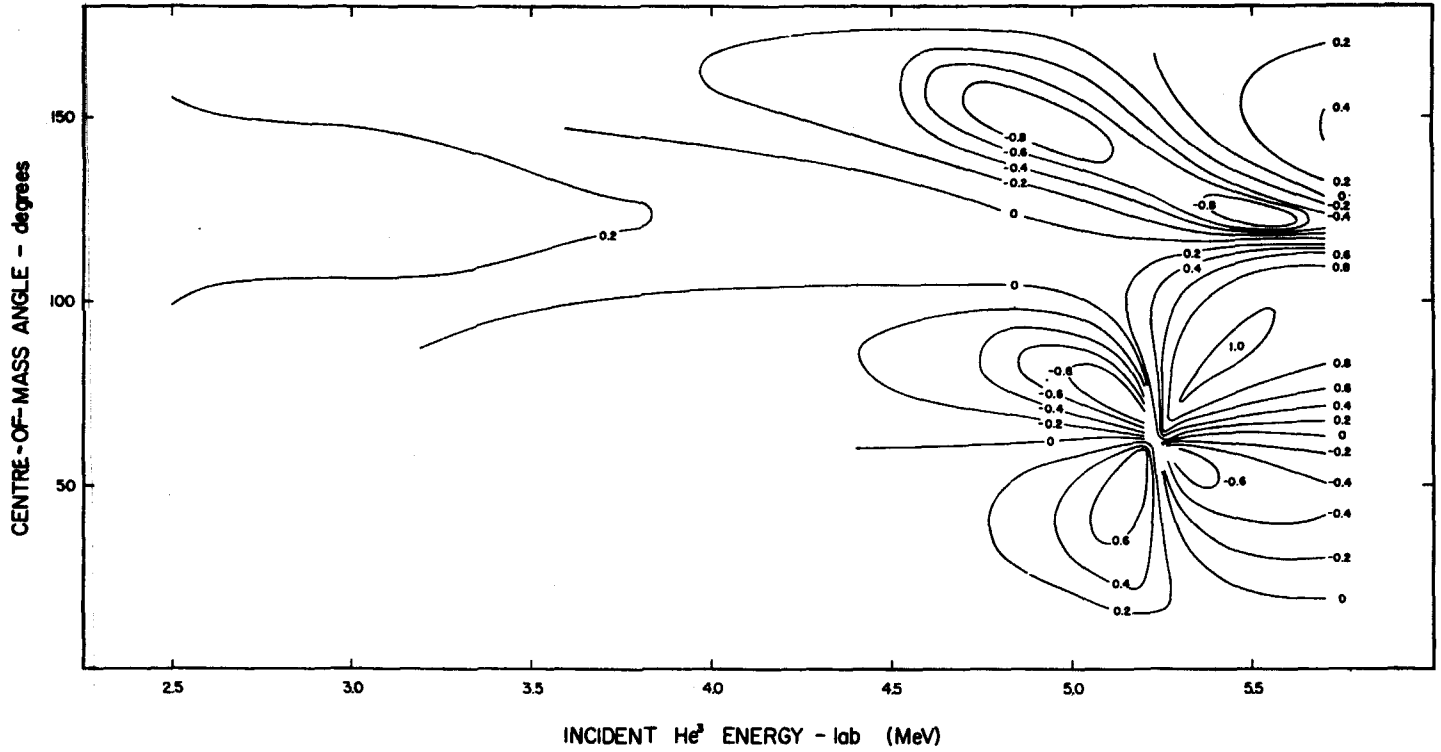

Fig. 7. Map of spin polarization (Basel convention) calculated from the set B phase shifts.

will be called set A, having δ_1^- larger (closer to 180°) than δ_1^+. This follows the earlier analyses [1,2]). However, with this sign of P-wave splitting it was not found possible to obtain a good fit to the experimental cross sections in the region of the $E_x = 4.57$ MeV anomaly. The "best fits" were not very good, and to obtain them the P-wave phase shifts had to be allowed to vary with energy in an undesirable way, i.e., there was a strong tendency for the splitting to be reversed in sign close to the resonance energy. The same tendency can be seen in the phase shifts of Miller and Phillips [2]) and, close to the resonance energy of the $\frac{1}{2}^-$, $E_x = 6.51$ MeV state, in the phase shifts of Tombrello and Parker [1]).

A second set of phase shifts was therefore obtained, and will be called set B. In this set, δ_1^+ is larger than δ_1^- through the whole energy range investigated. Other differences between the two sets are small. The cross sections calculated from set B are shown as solid curves in figs. 2-3 and are seen to fit the experimental cross sections very well. The dash-dot curves on some of figs. 2-3 are the Rutherford scattering cross sections. Fig. 4 shows the S- and P-wave phase shifts of set B, and it can be seen that the P-wave phase shifts vary smoothly with energy. Fig. 5 shows the F-wave phase shifts of this set.

It should be emphasized that, except in the anomalous region, the set A phase shifts fit the experimental cross sections just as well as do the set B. In fig. 6 those P-wave set A phase shifts which give a good fit are shown as circles. The triangles in the anomalous region are interpolations, imposing a reasonable energy variation on the P-wave phase shifts. The cross sections calculated from the set A in the anomalous region are shown as dashed curves in fig. 2. It can be seen that set A gives cross sections which do not agree well with experiment in this region, so that the set B phase shifts are preferred on these grounds.

The spin polarization of the scattered He^3 particles has been calculated for both sets of phase shifts. For set B, a polarization map (Basel convention) is shown as fig. 7. The corresponding map for set A is not shown, but is indistinguishable from fig. 7 in the anomalous region, where the polarization is dominated by the large F-wave splitting. In fact, in this region fig. 7 is very similar to the map published by Phillips and Miller [6]), except for a reversal of the sign convention. Phillips *et al.*[7]) have measured the polarization under experimental circumstances corresponding to $\theta_{c.m.} = 77°$, $E_{He^3} = 4.9$ and 5.5 MeV. These experimental polarizations agree with those calculated in ref. [6]) and in this paper, confirming once more the $E_x = 4.57$ MeV state in Be^7 as $\frac{7}{2}^-$, and not $\frac{5}{2}^-$.

In the energy region below the anomaly, the F-wave splitting becomes small and the polarization is governed by the splitting of the P-wave phase shifts. Sets A and B give polarizations opposite in sign and thus a polarization measurement would unambiguously decide between them. Such a measurement is planned.

5. Discussion of the Phase Shifts

In figs. 4 and 5 various theoretical curves are shown for comparison with the experimental phase shifts. In the upper part of fig. 4 the solid curves are the S-wave

hard-sphere scattering phase shifts for radii $R = 2.7$, 2.9 and 3.1 fm. Since the accuracy of the experimental S-wave phase shifts is estimated as $\pm 2°$, there is fair agreement with hard-sphere scattering for a radius of about 2.8 fm. However, there is some systematic tendency for the experimental phase shifts to become less negative than this at the higher energies of the present experiment. This tendency persists at higher energies [1]) and would be consistent with the existence of a high-lying S-state in Be^7.

The curves in the lower part of fig. 4 are calculated P-wave phase shifts. Curve (a) is for hard sphere scattering (with 180° added) with $R = 3.8$ fm and does not fit the experimental phase shifts. The experimental δ_1^+ phase shifts are well fitted by curve (b). This curve was calculated from single-level dispersion theory (using the expressions given, for instance, in refs. [2, 4])) including the effect of the Be^7 ground state. The parameter values were $R = 3.8$ fm, $\theta_{gs}^2 = 0.15$. Here θ_{gs}^2 is the reduced width of the ground state in units of the Wigner limit. Since the resonance energy of this state is known to be -1.587 MeV, the above parameters also determine the characteristic energy of the state.

Curve (c) is a calculated δ_1^- curve, including the effect of the first excited state in Be^7. The parameter values were $R = 3.8$ fm, $\theta_1^2 = 1.0$. It can be seen that this curve does not fit the experimental points. The effect of changing the parameters is roughly as follows: reducing either R or θ_1^2 reduces the slope of the curve and raises it on the graph. It can therefore be seen qualitatively that a fit to δ_1^- cannot be obtained; if a curve with the right slope is obtained, it lies too high on the graph. Calculations were made in the range $2.5 \leqq R \leqq 4.2$ fm, $0 \leqq \theta_1^2 \leqq 10$ without producing even a poor fit. For instance, the dashed curve in fig. 4 was calculated for $R = 2.8$ fm, $\theta_1^2 = 2.0$.

It appears that the values of δ_1^- obtained from this experiment cannot be explained by the influence of the first excited state of Be^7 alone. However, the discrepancy is such that the introduction of a high-lying $\frac{1}{2}^-$ state in Be^7 would improve the fit. This speculation will not be pursued in the present paper.

The experimental and theoretical F-wave phase shifts appear in fig. 5, where the solid curve is a fit to the δ_3^+ phase shift calculated from dispersion theory using a single $\frac{7}{2}^-$ level in Be^7. A radius of 4.4 fm was used to permit a direct comparison with

TABLE 2

Parameters of states in Be^7

	J^π	R (fm)	$E_J{}^\pi$ (MeV)	E_x (MeV)	$\gamma^2{}_J{}^\pi$ (MeV)	Ratio to Wigner limit
Ground state ($\delta_1{}^+$)	$\frac{3}{2}^-$	3.8	-1.986	0.0	0.38	0.15
Second excited state	$\frac{7}{2}^-$	4.4	3.56	4.57 ± 0.04	0.7 ± 0.1	0.38 ± 0.05
Third excited state [a])	$\frac{5}{2}^-$	4.4		6.51 ± 0.04		0.48

[a]) From ref. [1]).

the results of Miller and Phillips [2]). The values of the parameters used here are shown in table 2 and agree well with their values. Slightly better agreement with the experimental phase shifts can be obtained by using a smaller radius.

The authors gratefully acknowledge many fruitful discussions with Dr. T. A. Tombrello and Dr. F. S. Levin. They also thank Mr. Jeff D. Bronson, Jr., and Miss Anne E. Pitts for the energy calibration work, and the A & M College of Texas Data Processing Center for allowing the use of their IBM 709 computer at nominal cost.

References

1) T. A. Tombrello and P. D. Parker, Phys. Rev. **130** (1963) 1112
2) P. D. Miller and G. C. Phillips, Phys. Rev. **112** (1958) 2048
3) C. M. Jones, G. C. Phillips, R. W. Harris and E. H. Beckner, Nuclear Physics **37** (1962) 1
4) A. C. L. Barnard, C. M. Jones and J. L. Weil, Nuclear Physics **50** (1963) 604
5) K. F. Famularo and G. C. Phillips, Phys. Rev. **91** (1953) 1195
6) G. C. Phillips and P. D. Miller, Phys. Rev. **115** (1959) 1268
7) G. C. Phillips, R. R. Perry, P. M. Windham, G. K. Walters, L. D. Schearer and F. D. Colegrove, Phys. Rev. Lett. **9** (1962) 502